International Journal of Research in Engineering and Innovation (IJREI)
journal home page: http://www.ijrei.com
ISSN (Online): 2456-6934

Implementation of a shunt active power filter for power quality improvement: Harmonic compensation and power factor correction

Emmanuel Hernández[1], Efraín Dueñas[1], Reynaldo Iracheta[1], Hugo J. Cortina[1], Miguel A. Hernández[2]

[1]*Division of graduate studies, University of Isthmus. Av Universitaria s/n. Tagolaba. Tehuantepec, Oaxaca, México*
[2]*Fondo Sener-Conacyt-Sustentabilidad Energética and CEMIE-Eólico*

Abstract

A harmonic analysis at a point in the substation of Santo Domingo Tehuantepec, near the University of Isthmus in Oaxaca, Mexico, where the harmonic voltage distortion level exceeds the limit established by the Energy Regulation Commission (CRE) is analyzed. For this purpose, the implementation of a passive filter is proposed as a strategy of harmonic compensation where, through a capacitors bank that it possesses, power factor correction is allowed, considering the electrical characteristics of the grid, as well as the resonance points present in it, in order to avoid possible damage to the filter components and to insert unwanted extra resonance levels into the grid under study. Using the MATLAB/Simulink® software, the system was simulated to corroborate the response after connecting the filter, obtaining satisfactory results thanks to careful tuning of the proposed strategy.

Key words: Harmonic analysis, Energy Regulation Commission (CRE), passive filter, harmonic compensation, resonance levels.

1. Introduction

In electrical power systems, unwanted currents and voltages are common. These are mainly due to the presence of loads that include electronic switching devices for their operation: commonly called non-linear loads, causing problems in them; like the protections bad behavior, increase in the losses by active power, deterioration in isolations and dielectrics, decrease in the useful life of the domestic appliances, among others. Such unwanted currents or voltages are called harmonic signals, which are linked to the waveform of voltage and current causing distortion in this, due in large part to the use of equipment that bases its operation on electronic devices that perform commutations at high frequency in its rated operating condition. In accordance with the legal attributions, the CRE, entity in charge of the regulatory legal framework that governs the companies that provide public utilities in México, is based on resolution 024 of the year 2005 [1], based on the stipulated, the Voltage Total Harmonic Distortion (THD_v) for voltage levels 1, 2 and 3 cannot exceed 5% [2]. University of Isthmus made measurements of the harmonic content in its voltage signal corroborating that at some points the THD_v exceeded the limit stipulated by the standard, which is why it is necessary to analyze and design a strategy to compensate for the excess. For this purpose, the implementation of a active filter is proposed as a compensation strategy, analyzing the behavior of the grid impedance as a function of frequency, so that, after incorporating the filter to the same, this behavior is not affected by the appearance of series or parallel resonances that contribute to the deterioration in the filter components and the same system.

2. Shunt Active Power Filter

Shunt active power filter based on voltage source converter (VSC) is an effective solution to current harmonics, reactive power and current unbalance. The basic principle of this filter is to use power electronics technologies to generate particular currents components that can cancel the current harmonic components from nonlinear load [3-5].
The performance of the shunt active filter depends on the reference compensating current detection algorithm and the current control technique used to drive the gating pulses of the active power filter switches to generate compensating current that should be injected into the power system to mitigate the current harmonics and compensate the reactive power [6-10].

Corresponding author: Emmanuel Hernández
Email Id: emanuel.mayoral7@gmail.com

The compensation characteristics of the shunt APF are shown in Fig. 1.

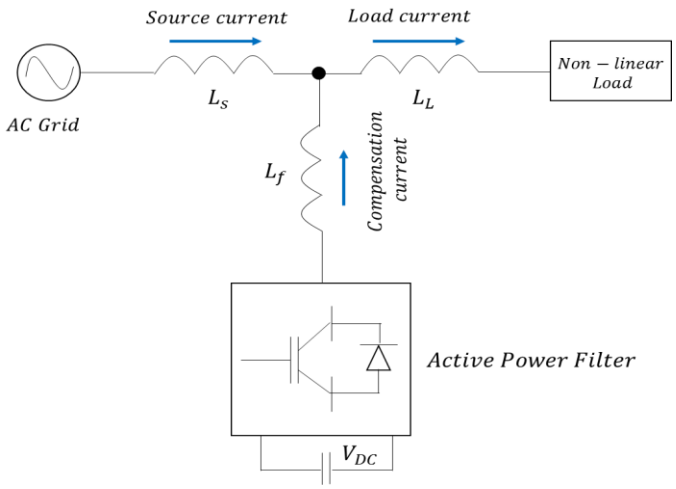

Figure 1. Basic configuration of a shunt active filter.

3. Instantaneous reactive power theory

Nowadays, modern notation is being used in polyphase electrical systems (see Fig. 2), where instantaneous voltages and instantaneous currents are expressed as spatial vectors. In an n-phase system the spatial vectors of voltage and current are given by:

$$\vec{v} = \begin{bmatrix} v_1 \\ v_2 \\ \vdots \\ v_3 \end{bmatrix}; \qquad \vec{\imath} = \begin{bmatrix} i_1 \\ i_2 \\ \vdots \\ i_3 \end{bmatrix} \tag{1}$$

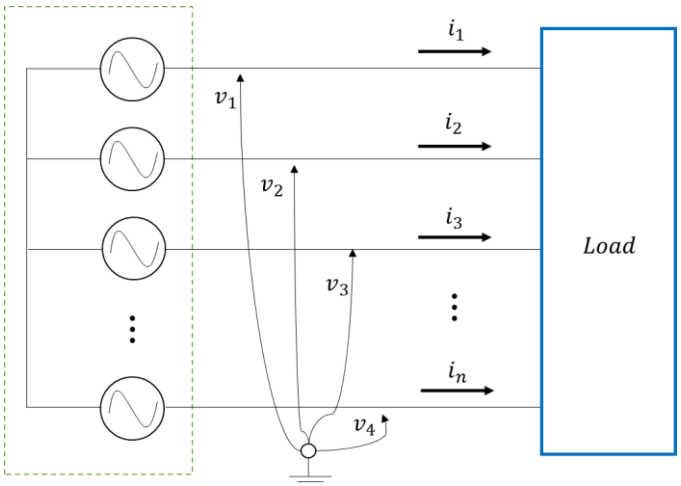

Figure 2. Electrical system of "n" phases.

The proposed formulation uses the vector representation of voltage and current to define a new expression of instantaneous power, called "instantaneous power tensor" [11].
This expression is obtained by the tensor product between the voltage and current vectors as follows:

$$\wp_{ij} = \vec{v} \otimes \vec{\imath} = \vec{v}\,\vec{\imath} \tag{2}$$

Where, $\mathscr{p}ij$ is the instantaneous power tensor and the superscript *t* refers to the transposition operator. Therefore, by replacing (1) in (2), the instantaneous power tensor is equal to:

$$\wp_{ij} = \begin{bmatrix} v_1 i_1 & v_1 i_2 & \dots & v_1 i_n \\ v_2 i_1 & v_2 i_2 & \dots & v_2 i_n \\ \vdots & \vdots & \ddots & \vdots \\ v_n i_1 & v_n i_2 & \dots & v_n i_n \end{bmatrix} \tag{3}$$

On the other hand, by applying the transposition operator in (2) the transposed instantaneous power tensor is obtained, thus:

$$\wp_{ij} = (\vec{v}\,\vec{\imath}) = \vec{v}\,\vec{\imath} = \vec{\imath} \otimes \vec{v} \tag{4}$$

This expression implies that the current vector can be obtained from the definition of the instantaneous power tensor as follows:

$$\vec{\imath} = \frac{\wp_{ij}}{\|\vec{v}\|^2}\vec{v} \tag{5}$$

Here $\|\cdot\|$ denotes the Euclidean norm of vectors. Now, starting from the next equality

$$\wp_{ij} = \wp_{ij} + \left(\wp_{ij}^t - \wp_{ij}\right) \tag{6}$$

and by replacing (6) in (5), the current vector can be expressed as:

$$\vec{\imath} = \frac{\wp_{ij}}{\|\vec{v}\|^2}\vec{v} + \frac{\wp_{ij}^t - \wp_{ij}}{\|\vec{v}\|^2}\vec{v} \tag{7}$$

The first term is the instantaneous active current:

$$\overrightarrow{\imath_p} = \frac{\wp_{ij}}{\|\vec{v}\|^2}\vec{v} = \frac{1}{\|\vec{v}\|^2}\begin{bmatrix} v_1 i_1 & v_1 i_2 & \dots & v_1 i_n \\ v_2 i_1 & v_2 i_2 & \dots & v_2 i_n \\ \vdots & \vdots & \ddots & \vdots \\ v_n i_1 & v_n i_2 & \dots & v_n i_n \end{bmatrix}\begin{bmatrix} v_1 \\ v_2 \\ \vdots \\ v_n \end{bmatrix}$$

$$= \frac{1}{\|\vec{v}\|^2}\begin{bmatrix} v_1 i_1 v_1 & + & v_1 i_2 v_2 & + & \dots & + & v_1 i_n v_n \\ v_2 i_1 v_1 & + & v_2 i_2 v_2 & + & \dots & + & v_2 i_n v_n \\ \vdots & & \vdots & & \vdots & & \vdots \\ v_n i_1 v_1 & + & v_n i_2 v_2 & + & \dots & + & v_n i_n v_n \end{bmatrix}$$

$$= \frac{(v_1 i_1 + v_2 i_2 + \cdots + v_n i_n)}{\|\vec{v}\|^2}\begin{bmatrix} v_1 \\ v_2 \\ \vdots \\ v_n \end{bmatrix} \tag{8}$$

This term represents the projection of the current vector on the voltage vector. Therefore, from (7) and (8), the instantaneous reactive current is expressed as follows:

$$\vec{\imath}_q = \frac{\wp_{ij}^t - \wp_{ij}}{\|\vec{v}\|^2}\vec{v} = \frac{\wp_{ij}^t}{\|\vec{v}\|^2}\vec{v} - \frac{\wp_{ij}}{\|\vec{v}\|^2}\vec{v} = \vec{\imath} - \vec{\imath}_p \quad (9)$$

This term represents the quadrature component with respect to the voltage vector. In a similar way to that established in [12], with these two currents, the traditional concepts of instantaneous power can be defined. This is how the conventional instantaneous active power in *n*-phase systems can be defined as the scalar product between the instantaneous active voltage and current vectors, thus:

$$p = \langle \vec{v} \cdot \vec{\imath}_p \rangle \quad (10)$$

The instantaneous tensor of imaginary power defined by the tensor product between the voltage vectors and instantaneous reactive current.

$$q_{ij} = \vec{v} \otimes \vec{\imath}_q \quad (11)$$

Allows to calculate the norm of instantaneous imaginary power, like this:

$$q = \|q_{ij}\| = \|\vec{v}\| \cdot \|\vec{\imath}_q\| \quad (12)$$

4. Research method

The data used for this study are records taken at the point that has the name TEH-C1, this is the main switch of the transformation module of 25-32MVA located in the substation of Tehuantepec; this is a point of 13.2kV. These measures were carried out between the periods of August 1 to September 1, 2014. The readings were taken from 12:00 hours on August 1 until 12:00 hours on September 1, every 10 minutes being carried out measurement of the harmonic levels present in each of the phases in the point. According to the 4465 records, the highest level of THD_v in the grid was chosen as the study base; based on this, it was modeled using the software MATLAB/Simulink®, which through the harmonic current injection method [13] allowed the simulated harmonic spectrum to be as close as possible to the data measured in reality, this with the purpose of prospectively analyzing the levels of THD_v present in the grid after the strategy implementation, so that they were in the values recommended by the CRE.

5. Results and Discussions

5.1. Preliminary analysis and data validation

A preliminary analysis of the records was carried out in order to determine the event where the highest level of $THDv$ was presented and, further the compensation strategy to be used. This took place on August 8 at 4:30 p.m. where the level of $THDv$ for phase A, B and C was 5.0246%, 5.4571% and 5.3931%, respectively. As shown in Table I showing $THDv$ levels, in Table II the total harmonic current distortion ($THDi$) levels. Based on the data obtained, it was analyzed that the 5th harmonic affects notably so that the THD_v exceeds the levels, not only this record, but in all, since it is the harmonic with the highest-level present in all the measurements made (see tables III, IV and V).

Table 1: Registered THD_v Level (08/12/2014)

Harmonic *(h)*	Phase A *(%)*	Phase B *(%)*	Phase C *(%)*
1	100	100	100
3	0.2711	0.7033	0.4421
5	4.9622	5.3745	5.3209
7	0.5643	0.5447	0.4530
9	0.0317	0.0736	0.0467
11	0.1580	0.1563	0.1045
13	0.0828	0.0951	0.1074

Table 2: Registered THD_i Level (08/12/2014)

Harmonic *(h)*	Phase A *(%)*	Phase B *(%)*	Phase C *(%)*
1	100	100	100
3	0.1007	0.2622	0.2158
5	2.5536	3.3732	2.8978
7	1.1431	1.0676	1.2346
9	0.0193	0.1563	0.1442
11	0.5664	0.5182	0.5657
13	0.2185	0.2279	0.2033

When examining the situation that presents itself, attacking the 5th harmonic would cause the THD_v to decrease considerably, since it is the one with the greatest influence so that the level exceeds its limit. Based on what has been proposed, the compensation strategy for active filtering is adapted to our study case, since it is possible to tune a filter to the 5*th* harmonic frequency (300 Hz).

Table 3: High and Low Harmonic Levels in "Phase A"

Harmonic *(h)*	$THD_v(\%)$ max	$THD_v(\%)$ min	$THD_v(\%)$ $average$
3	0.1007	0.2622	0.2158
5	2.5536	3.3732	2.8978
7	1.1431	1.0676	1.2346
9	0.0193	0.1563	0.1442
11	0.5664	0.5182	0.5657
13	0.2185	0.2279	0.2033

Table 4: High and Low Harmonic Levels in "Phase A"

Harmonic *(h)*	$THD_v(\%)$ max	$THD_v(\%)$ min	$THD_v(\%)$ $average$
3	0.99262	0.2638	0.5549
5	5.3745	0.9527	2.1750
7	0.9435	0.0335	0.2604
9	0.1503	0.0321	0.0894
11	0.2512	0.0022	0.0615
13	0.1565	0.0090	0.0722

Table 5: High and Low Harmonic Levels in "Phase A"

Harmonic *(h)*	$THD_v(\%)$ max	$THD_v(\%)$ min	$THD_v(\%)$ $average$
3	0.5678	0.1918	0.3436
5	5.3209	0.91112	2.1969
7	0.9470	0.228	0.2331
9	0.0981	0.0154	0.0477
11	0.2299	0.0155	0.0759
13	0.1832	0.0171	0.0753

This is to facilitate the passage of these through of a path of low impedance that would be formed in the branch to be designed. Through MATLAB/Simulink®, the grid was modeled (see Fig. 3), obtaining levels of THD_v very close to the values measured in reality.

5.2. Design and tuning of the active filter

Shunt or parallel active filters provide a path of low impedance for harmonic currents, is composed of a RLC branch in series, which is connected in parallel with the bar or power system. Besides being more economical than other compensation strategies and transporting only the currents for which it was tuned, there is a possibility that it provides part of the reactive power of the system [14]. The impedance of the filter to be designed is:

$$Z = R_F + j\left[\omega L_F - \frac{1}{\omega C_F}\right] \quad (13)$$

Where:
ω: Angular frequency
R_F: Filter resistance
L_F: Filter inductance
C_F: Filter capacitors bank

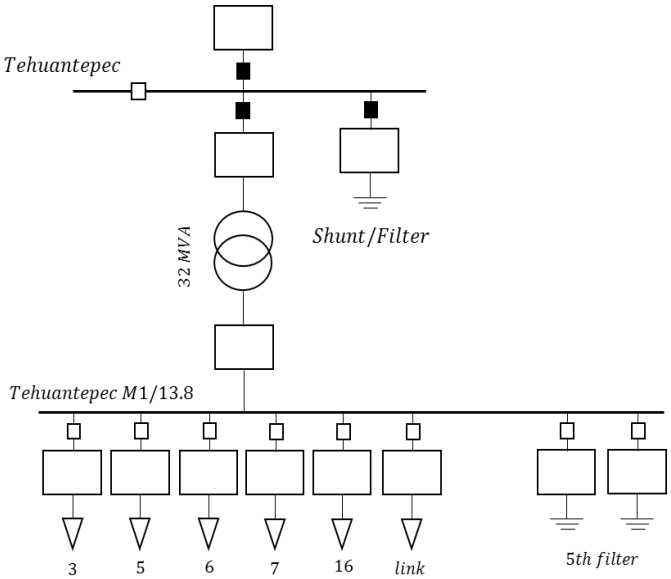

Figure 3. Single-line diagram of the TEH-C1 point using MATLAB/Simulink

Its structure and frequency response are shown in Fig. 4. Based values of the system: $MVA_{base} = 11.141\ MVA, kVA_{base} = 13.8\ kV$. So, $Z_{base} = (kVA_{base})^2/MVA_{base} = (13.8)^2/11.4 = 17.0936\ \Omega$. This is the filter calculation to eliminate the 5*th* harmonic (tuning performed at 6% less than the harmonic frequency, according to the IEEE-1531-2003 standard) [15]. When making the measurements, the power factor of the system was 0.827. For the design it is proposed that it is wanted to raise the same to 0.95, based on antecedents that show that to justify the investment, at least the power factor must be raised to this value. Therefore, the power in the capacitor (16) must be:

$$\theta_n = cos^{-1}(PF_n) \quad (14)$$

Then, $\theta_1 = cos^{-1}(PF_1) = cos^{-1}(0.827) = 34.2082°$ and $\theta_2 = cos^{-1}(PF_2) = cos^{-1}(0.950) = 18.995°$. Therefore,

$$\theta_{eff} = P(\tan\theta_1 - \tan\theta_2) \quad (15)$$

Therefore, $\theta_{eff} = 9.35MV[\tan(34.2082) - \tan(18.995)] = 3.099\ MVA_r$. The three-phase capacitor bank installed in point TEH-C1 must be selected with respect to the commercial values established in the IEEE-18-2002 standard [16]. The arrangement will consist of one group per phase, such group will in turn have 5 units of 200 $kVAr$ capacitors, making a total of 1 $MVAr$ per phase and 3 $MVAr$ three-phase. The grid impedance to the fundamental frequency is calculated, as well as the capacitive impedance, the capacitance, the inductive impedance and the inductance according to (16–20).

$$X_{eff} = \frac{(V_{LL-syst})^2}{Q_{eff}} = \frac{(13.8\ kV)^2}{3\ MVA} = 63.48\ \Omega \quad (16)$$

$$X_C = \frac{h^2}{h^2-1} X_{eff} = \frac{(4.7)^2}{(4.7)^2-1} 63.48 = 66.50\ \Omega \quad (17)$$

$$C = \frac{1}{2\pi f X_C} = \frac{1}{2\pi(60)(66.5)} = 39.8\ \mu F \quad (18)$$

$$X_L = \frac{X_L}{h^2} = \frac{66.5\Omega^2}{(4.7)^2} = 3.0104\ \Omega \quad (19)$$

$$L = \frac{X_L}{2\pi f} = \frac{3.0104\ \Omega}{2\pi(60)} = 7.9853\ mH \quad (20)$$

For this type of filters [17] it is recommended that the quality factor has a value between 20 and 30. In the present design we have a value of 20, $R = X_L(f_{reson})/Q_f = 3.01(4.7)/20 = 0.7074\ \Omega$. For the filter to have a path of low impedance at the required frequency, it must be fulfilled that:

$$X_C = X_L \quad (21)$$

$X_C(h = 4.7) = X_C/h = 66.5\Omega/4.7 = 14.148\Omega$ and $X_L =$

$(h = 4.7) = hX_L = 4.7(3.0104\ \Omega) = 14.1489\ \Omega$. To verify that the filter is not damaged by possible overcurrent's due to harmonic currents, it is corroborated that it does not exceed 135% of the fundamental current, as established by the IEEE-18-2002 standard. $I_3 = 0.2622\%\ I_{fund} = 0.334\ A;\ I_5 = 3.37\ I_{fund} = 4.3737\ A;\ I_7 = 1.067\ I_{fund} = 1.384\ A;\ I_9 = 0.156\%\ I_{fund} = 0.2027\ A;\ I_{11} = 0.5182\ I_{fund} = 0.6719\ A;\ I_{13} = 0.228\%\ I_{fund} = 0.2955\ A.$

$$I_{total\ RMS} = \sqrt{I_1^2 + I_3^2 + I_5^2 + I_7^2 + I_9^2 + I_{11}^2 + I_{13}^2} \quad (22)$$

$$\%current\ margin = \frac{I_{total\ RMS}}{I_{total\ fund(1)}} \times 100 = 100.69\% \quad (23)$$

$$I_{total\ RMS} = 1.00069\ I_{fund}(1) < 1.35 I_{fund}(1) \quad (24)$$

Now it is checked that the peak voltage of the system does not exceed the design voltage of the capacitor bank; it is corroborated that this does not exceed 120% of the peak phase voltage of the system, as established by the IEEE-18-2002 standard. Calculation of voltage at fundamental frequency.

$$V_C(1) = I_{fund}(1) X_C = 8.3452\ kV \quad (25)$$

Calculation of the voltages caused by the harmonics:

$$V_C(h) = \sum_h^n I(h) \frac{X_C}{h} \quad (26)$$

According to (25), we have: $X_C(3) = 0.334\ (66.5/3) = 7.4V$ $X_C(5) = 0.334(66.5/5) = 58.17V;\ X_C(7) = 1.38(66.5/7) = 58.17V;\ X_C(9) = 0.202(66.5/9) = 1.497V;\ X_C(11) = 0.6719(66.5/11) = 1.0619V;\ X_C(13) = 0.2955(66.5/13) = 1.5116V$. Therefore, $X_C(h) = 0.0858\ kV$. Calculation of the peak voltage per phase of the capacitor:

$$V_{C_{L-N\ peak\_total}} = \sqrt{2}[V_C(1) + V_C(h)] = 11.9232\ kV \quad (27)$$

$$\%peak\ voltage\ margin = \frac{V_{C\ L-N\ peak\ syst}}{V_{L-N\ peak\ syst}} \times 100 = 106\%$$

$$V_{C\ L-N\ peak\ total} = 1.0581\ V_{L-N\ peak\ total} < 1.2\ V_{L-N\ peak\ tot}$$

The peak voltage value complies with the IEEE-18-2002 standard. The RMS voltage of the system must not exceed the design RMS voltage of the capacitor bank (38); it is corroborated that this does not exceed 110% (40) to the RMS phase voltage of the system, as established by the IEEE-18-2002 standard. RMS voltage calculation of the capacitor is:

$$V_{C\ L-N\ RMS} = \sqrt{V_C(1) + V_C(3) + V_C(5) + V_C(7) + V_C(9) + V_C(11) + V_C(13)}$$

$$= 8.3454\ kV$$

Calculation of the RMS phase voltage of the system:

$$V_{C\ L-N\ RMS} = \frac{V_{L-L\ syst}}{\sqrt{3}} = 7.9674\ kV$$

$$\%RMS\ voltage\ margin = \frac{V_{C\ L-N\ RMS}}{V_{L-N\ RMS\ syst}} \times 100 = 104.74\%$$

$$V_{C\ L-N\ RMS} = 10474\ V_{L\ RMS\ total} \leq 1.1\ V_{L-N\ RMS\ syst}$$

The RMS voltage value complies with the IEEE-18-2002 standard. Reactive power is corroborated based on the norm:

$$Q_{3\varphi_{re}-calculated} = \frac{(V_{C\ L-N\ RMS})^2}{X_C} \times 3 = 3.1419\ MVA_r$$

$$\%VA_r\ margin = \frac{Q_{3\varphi_{re}-calculated}}{Q_{eff}} \times 100 = 104.73\%$$

The power value complies with the IEEE-18-2002 standard. To complete the design of the active filter, it is verified that the heating of the capacitor dielectric is acceptable based on the IEEE-18-2002 standard. This is evaluated by inequality:

$$\sum_h [V_C(h) I(h)] \leq 1.35\ Q_{3\varphi_{re}-calculated}$$

$$\{3[(8.34k \times 125.49) + (7.40 \times 0.33 + (58.17 \times 4.373))]\}$$
$$+(13.15 \times 1.384) \times \{(1.497 \times 0.202) + (4.06 \times 0.671)\}$$
$$+\{1.511 \times 0.295\} \leq (1.35 \times 3.1419\ MVA_r)$$

Comparing the inequality, we have:

$$3.1426\ MVA_r \leq 4.2616\ MVA_r$$

The inequality is satisfied, therefore the heating of the dielectric of the capacitor is acceptable.

5.3. Results of the simulation

The complete model of the system connected to the grid is shown in Fig. 4. The voltages are considered as a sinusoidal and balanced in the MATLAB/Simulink® simulation. The load current THD is found to be 27.88% when a switching power electronic load is considered. The parameters for voltage sources, transmission lines, filters and the load details are provided in the Table VI. The Shunt APF complete model is shown in the Fig. 5. When performing the injection of the harmonic currents measured at the TEH-C1 point (see Table II), harmonic levels very similar to reality were obtained (see Fig. 6).

Table 6: System Parameters Used in MATLAB/Simulink®

Simulation parameters	Values
Supply voltage (V_s)	13.2 kV (peak values)
System frequency (F_s)	50 Hz
Source impedance (R_s; L_s)	0.1 Ω; 0.15 mH
Filter impedance (R_c; L_c)	0.1 Ω; 0.15 mH
DC link voltage (V_{dc})	170 V
DC link capacitance (C_{dc})	200 μF
Optimal values (K_p and K_i)	0.2 and 9.32
Hysteresis band	$\pm 0.2\ A$
Load	Diode rectifier
Snubber resistance (R_{sn})	500 Ω
Snubber capacitance (C_{sn})	$250e^{-9}\ F$
Load impedance (R_l; L_l)	30 Ω; 20 mH

The source current for one of the three phases without compensator is shown in Fig.7. Simulations of the system show that at these conditions, parallel and series resonances are present, which are dangerous if one considers that such peaks are close to the fundamental frequency. Then, the behavior of the bar at high frequencies is clearly inductive. There is also a slight deformation in the voltage waveform for this point (see Fig. 8).

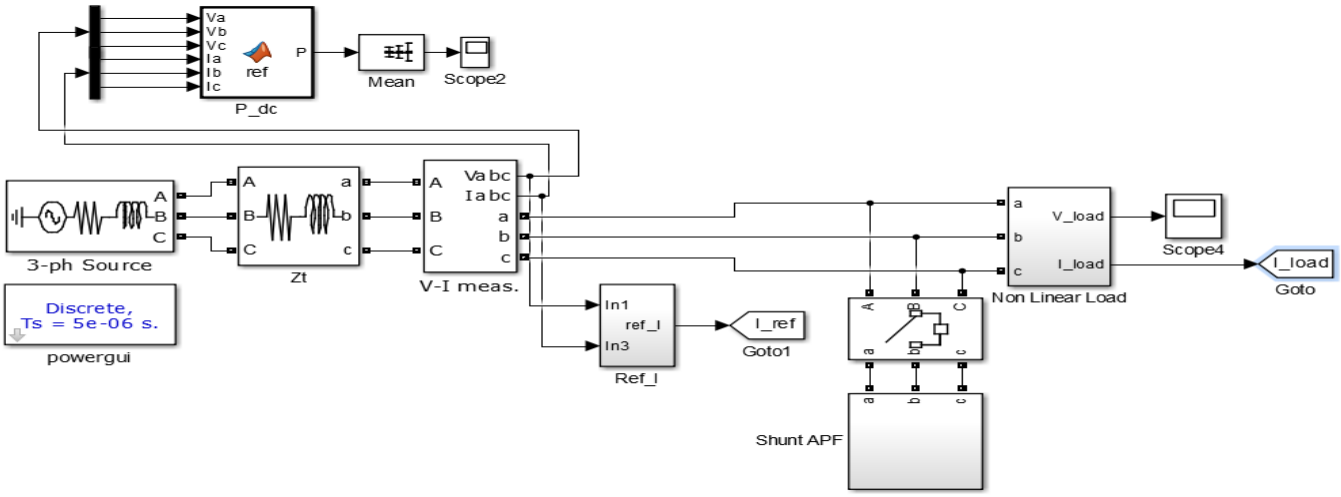

Figure 4. Complete model of the Non-Linear Load connected to grid without apply the Shunt Active Power Filter

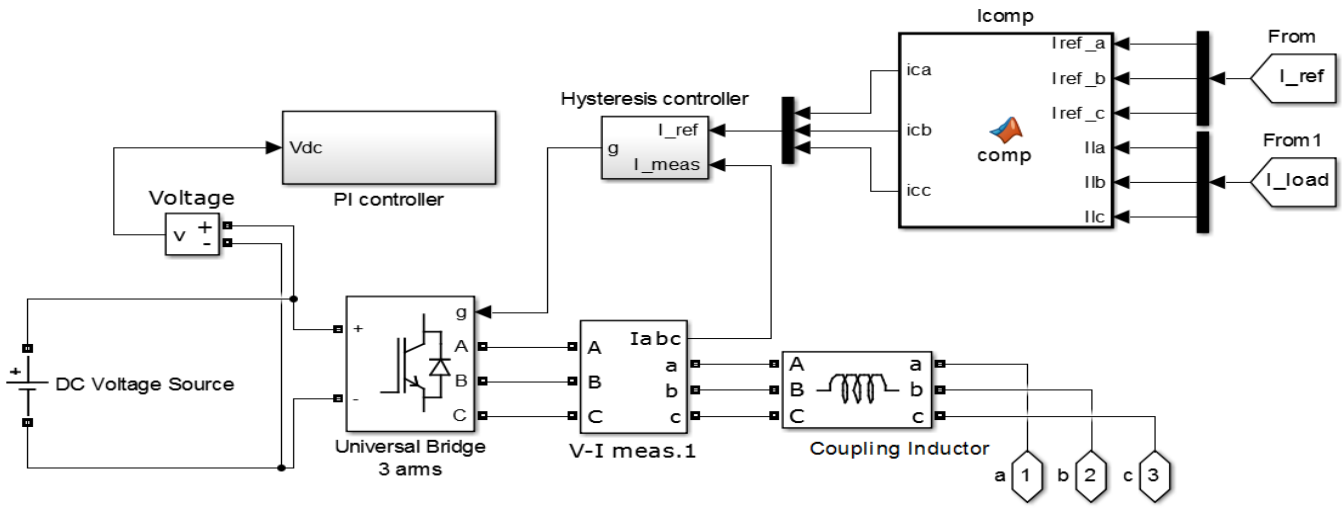

Figure 5. Shunt Active Power Filter model.

During, *t*=0.05 *s*, compensator is set to active mode (i.e., pulse applied for the inverter section). The source current, compensation current, and DC capacitor voltage for proportional-integral and Shunt APF have been illustrated from Fig. (7-12). Based on this model, we proceed to obtain the Impedance vs. Frequency curve of the bar at 13.2 *kV*.

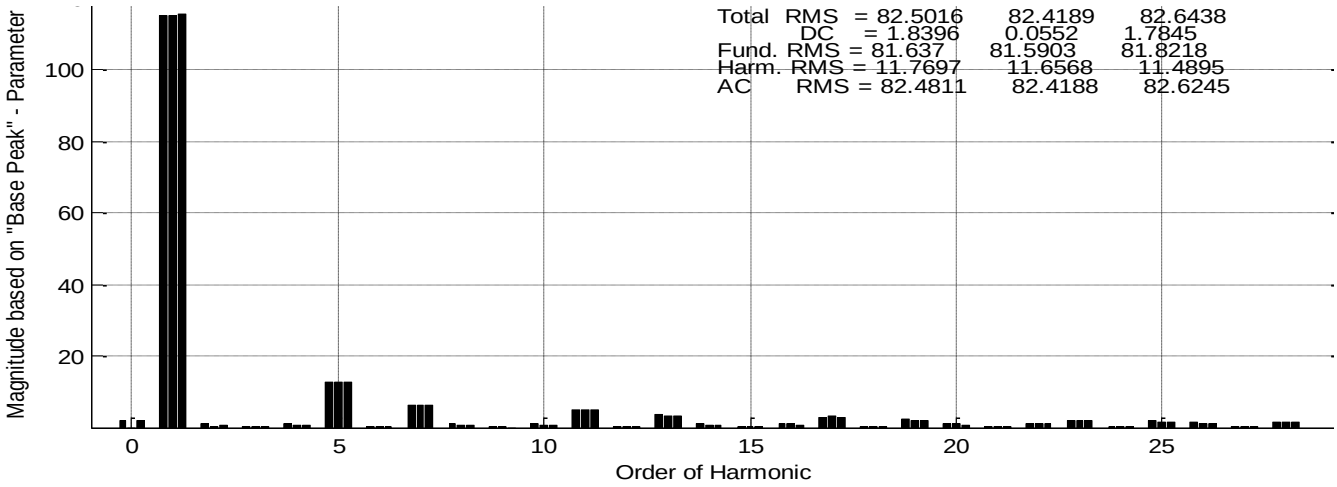

Figure 6. Levels of harmonics in the bar 2.

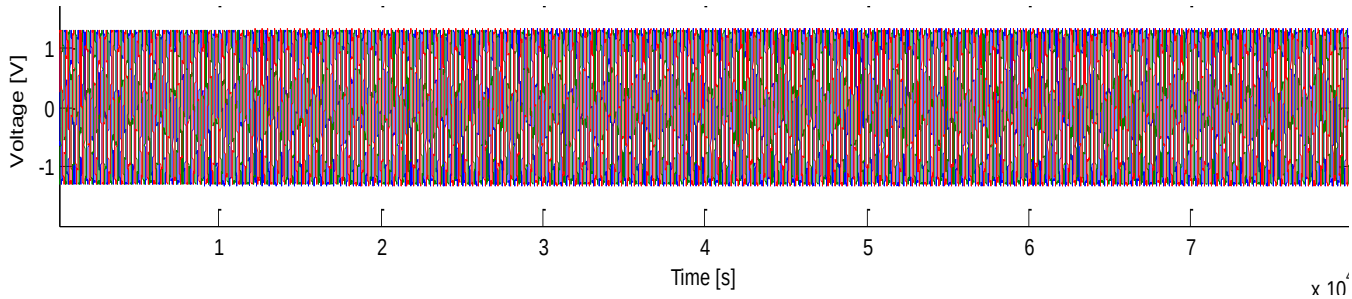

Figure 7. Three-phase voltages in TEH-C1 (Bar to 13.2 kV)

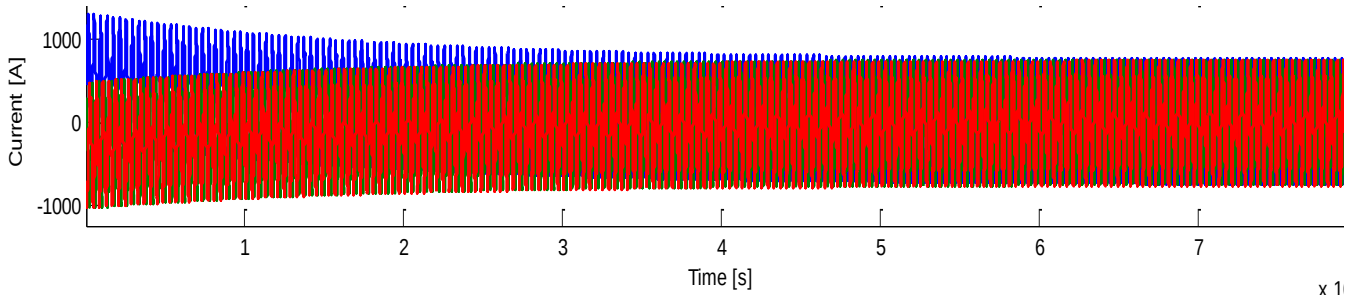

Figure 8. Three-phase currents in TEH-C1 (Bar to 560 A)

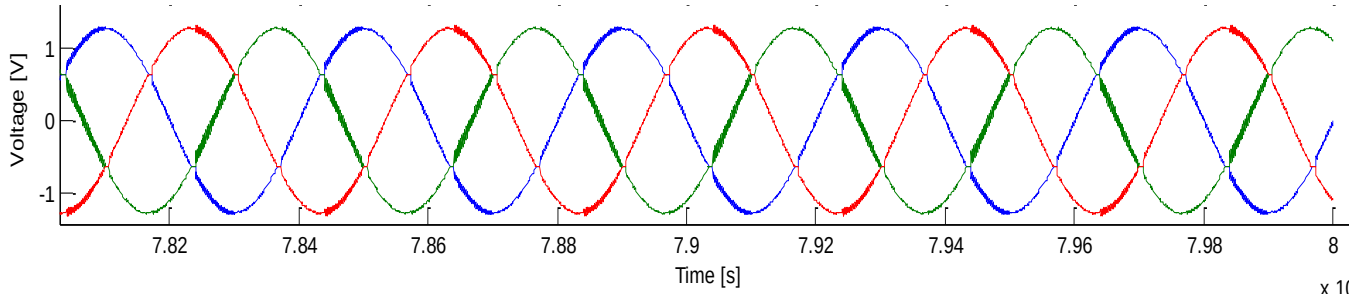

Figure 9. Zoom of Fig. 7.

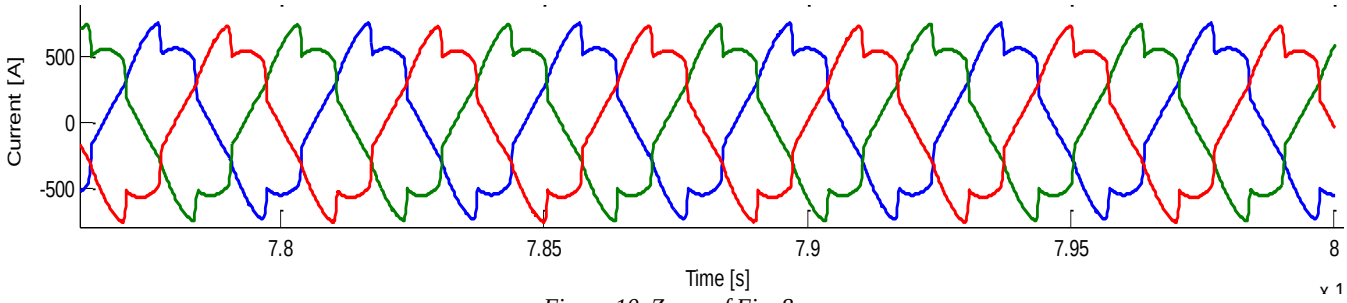

Figure 10. Zoom of Fig. 8.

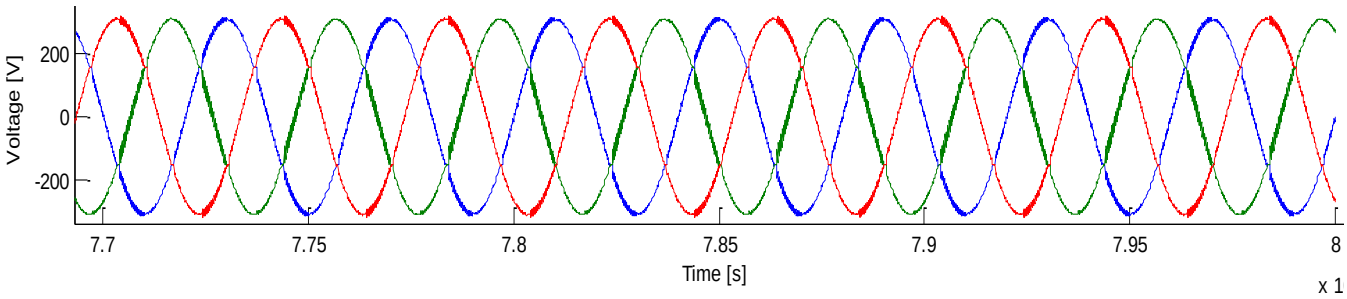

Figure 11. Three-phase voltages in load of the TEH-C1 (Bar to 300 V)

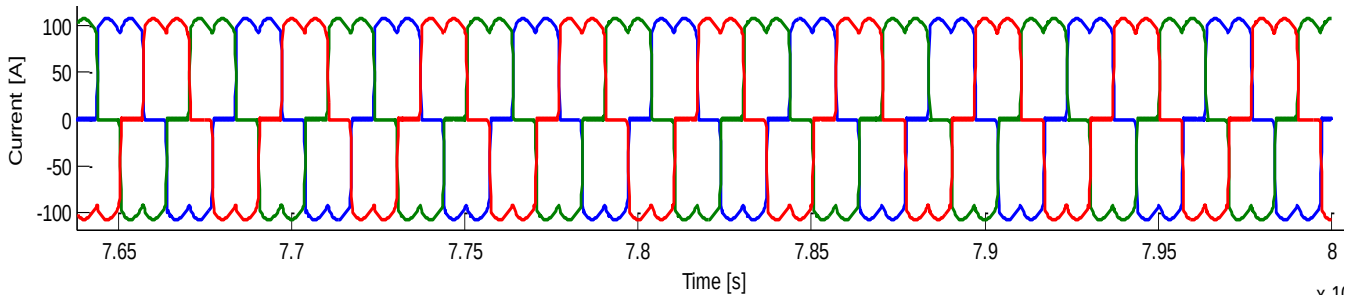

Figure 12. Three-phase currents in load of the TEH-C1 (Bar to 100 A)

5.4. Analysis of the incorporation of an active filter

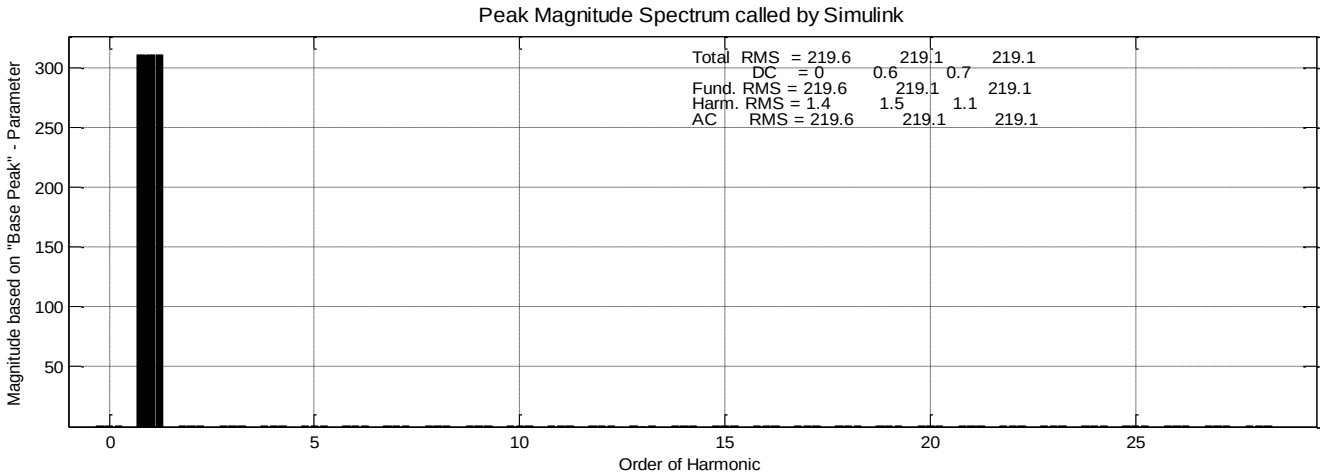

Figure 13. Levels of harmonics in the bar 2.

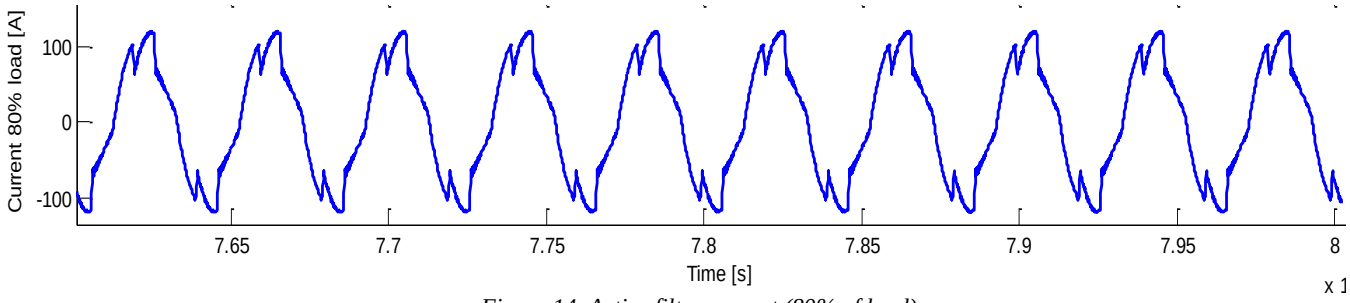

Figure 14. Active filter current (80% of load).

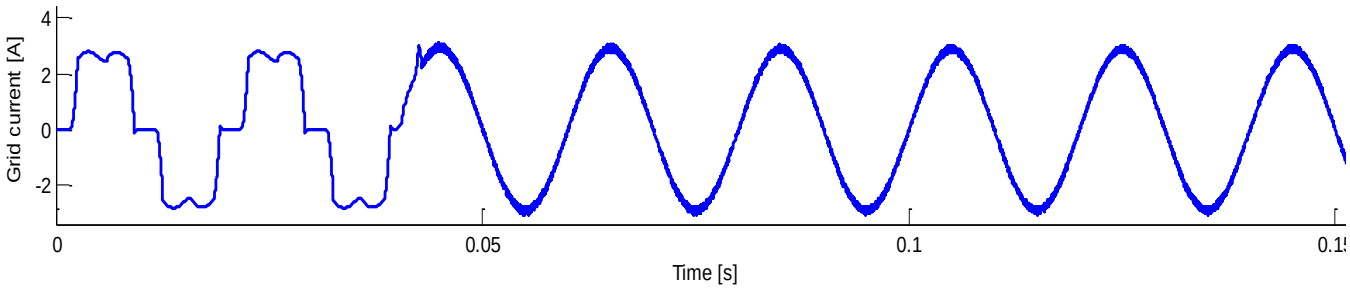

Figure 15. Grid current after incorporating the active filter.

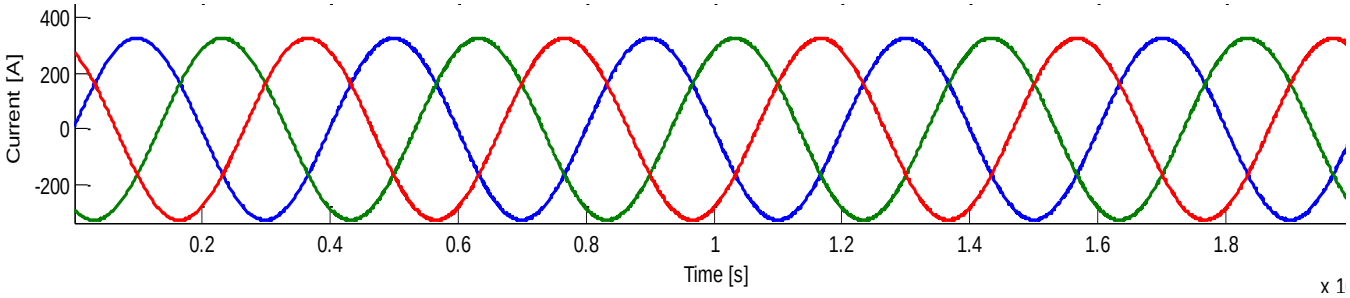

Figure 16. System current after incorporating the active filter.

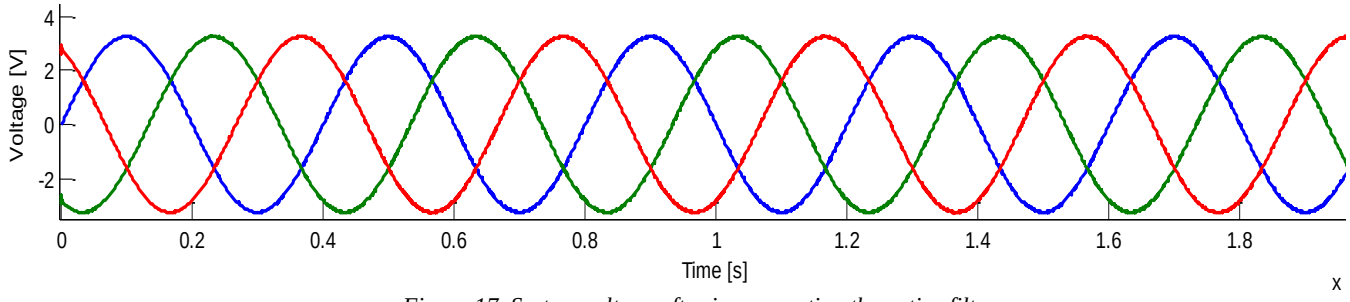

Figure 17. System voltage after incorporating the active filter.

Through the studies of harmonics made, based on the actual measurements of the load, the type of equipment that is convenient to use for compensation was determined. Depending on the possible resonances and the harmonic currents existing in the network, it is convenient to carry out the compensation with traditional passive equipment (bank of capacitors), with a pure active filter or the combination thereof with traditional compensation, hybrid. The minimum capacity requirements of an active filter will depend on the injection of reactive power at fundamental frequency and/or on the attenuation or elimination of the harmonic frequency currents of the network. With respect to the switching frequency of the filter design, it is observed that it is not high since the harmonics of interest of the load did not result from high frequencies.

This is favorable in terms of a high power or medium voltage design. Then, the filter is connected. The tuning was performed at a lower frequency than desired, in our case to eliminate the 5^{th} harmonic. It was tuned to a frequency 6% lower than the desired one (300Hz); that is to say to 282 Hz, since first, the polluting currents are not going to be exactly at the harmonic frequency, but at a lower frequency and, second, before a

change of the series resonance to values of high frequency, it will result in a increase in the impedance seen by the harmonic currents that are the order of the design frequency, causing wear on the filter components as the aging of the capacitor, which would cause its capacitance to decrease [17]. After the inclusion of the filter in the system, a considerable reduction in the level of harmonic distortion of the grid, approximately 71% (see tables VII and VIII).

Table 7: Level of harmonic after the inclusion of the filter

Harmonic (*h*)	Phase A *(%)*	Phase B *(%)*	Phase C *(%)*
1	100	100	100
3	0.5563	0.5563	0.5563
5	1.3818	1.3818	1.3811
7	0.4342	0.4348	0.4342
9	0.0004	0.0004	0.0004
11	0.1087	0.1087	0.1178
13	0.0730	0.0734	0.0737

Table 8: Comparison of THD_v after filter inclusion

Phase	Non-filter	Filter
A	5.7342	1.5571
B	5.3770	1.5573
C	5.3754	1.5571

An improvement in the voltage waveform is noted, resembling more a fully sinusoidal wave (see Fig. 11). It is appreciated how the inclusion of an active filter, tuned to the harmonic frequency that most affects the voltage signal, can be a possible solution to decrease the distortion present in the TEH-C1 point, where, in addition, it also contributes to raise the factor of system power to 0.95.

6. Conclusion

The compensation strategy through active filters is a good solution to reduce the harmonic distortion, in those cases where $THDv$ exceeds its level thanks to the fact that certain harmonics present a higher level than others in specific and this level is close to the allowed limit; for grids where THD levels are well above the norm, it is recommended to implement another compensation strategy. In addition, to reducing the harmonic content, it was also possible to include a capacitor bank design, which markedly affected the improvement in the power factor, where the reactive power necessary for such improvement is the basis in this case for the design of the filter. As a result of the high vulnerability that this type of strategy presents, it was necessary to perform a careful filter tuning, in order to avoid that with the time and conditions to which it is exposed, a slight variation in the frequency of design causes damage in the filter components. However, this dis-tuning with time is inevitable, due to the wastage to which these components are subjected due to the continuous operation of the system. One of the main design guidelines is based on trying that the peak resonances of the system are far from the fundamental frequency or that they are at frequencies whose harmonic order is not injected by the non-linear loads connected to the grid, thus avoiding problems of overvoltage's and overcurrent's that affect for example the solid insulation of the cables, the coils of the machines, aging in the capacitor filter, among others. A high-quality factor is responsible for the appearance of a prominent valley at the design frequency in the Impedance vs. Frequency curve, which is why the capture occurs at such a high harmonic content point. However, these filters can trap harmonic currents of nearby frequencies, by which the impact of these extra currents on the operation of the filter must be evaluated. It is recommended to adopt a low-quality factor in situations where the level of THD slightly exceeds the norm, otherwise it is recommended to adopt a high value, previously studying the possible consequences that such pattern leads to in the design.

The possible future implementation of the proposed strategy will help University of Isthmus comply with the limits established by the CRE, demonstrating in turn the interest in providing a good service to the user, complying with the provisions of the regulation and implementing strategies to correct the existing problems, confirming its status as a leading company in the provision of service at the regional level [17], [18], [19].

Acknowledgment

This group of researchers is grateful for all the support provided by the Fondo SENER-CONACyT Sustentabilidad Energética and the CEMIE-Eólico for the development of this investigation.

References

[1] Resolución 024-2005, por la cual se modifican las normas de calidad de la potencia eléctrica aplicables a los servicios de Distribución de Energía Eléctrica, México, CRE, 2005.

[2] IEEE Recommended Practices and Requirements for Harmonic Control in Electrical Power Systems, IEEE standard 519-1992, 1992.

[3] F. Z. Peng, "Application issues of active power filters," Ind. Appl. Mag. IEEE, vol. 4, no. 5, pp. 21–30, 1998.

[4] G. Adam, A. G. S. Baciu, and G. Livinţ, "a matlab-simulink approach to shunt active power filters," in 25th European Conference on Modelling and Simulation, 2011, vol. 6, no. Cd, pp. 2–7.

[5] M. Kale and E. Özdemir, "Harmonic and reactive power compensation with shunt active power filter under non-ideal mains voltage," Electr. Power Syst. Res., vol. 74, no. 3, pp. 363–370, Jun. 2005.

[6] A. G. Prasad and A. N. Kumar, "Comparison of Control Algorithms for Shunt Active Filter for Harmonic Mitigation," Int. J. Eng. Res. Technol., vol. 1, no. 5, pp. 1–6, 2012.

[7] Z. Chelli, R. Toufouti, A. Omeiri, and S. Saad, "Hysteresis Control for Shunt Active Power Filter under Unbalanced Three-Phase Load Conditions," J. Electr. Comput. Eng., vol. 2015, pp. 1–9, 2015.

[8] P. Rathika and D. Devaraj, "Fuzzy Logic – Based Approach for Adaptive Hysteresis Band and Dc Voltage Control in Shunt Active Filter," Int. J. Comput. Electr. Eng., vol. 2, no. 3, pp. 404–412, 2010.

[9] K. Sebasthirani and K. Porkumaran, "Efficient Control of Shunt Active Power Filter with Self- Adaptive Filter Using Average Power Algorithm," Int. J. Emerg. Technol. Adv. Eng., vol. 3, no. 5, pp. 3–8, 2013.

[10] C. Salim and B. M. Toufik, "Intelligent Controllers for Shunt Active Filter to Compensate Current Harmonics Based on SRF and SCR Control

[11] Strategies," Int. J. Electr. Eng. Informatics, vol. 3, no. 3, pp. 372–393, 2011.
[12] A.J. Ustariz. "Formulación de una Teoría Tensorial de la Potencia Eléctrica: Aplicaciones al Estudio de la Calidad de la Energía". Tesis para optar al grado de doctor. Universidad Nacional de Colombia. Manizales, Colombia. 2011. URL: http://www.bdigitalnal.edu.co/3578/1/armandojaimeustarizfarfan.2011.pdf.
[13] J.L. Willems. "A New Interpretation of the Akagi-Nabae Power Components for Nonsinusoidal Three-phase Situations". IEEE Transactions on Instrumentation and Measurement. Vol. 41, Issue 4, pp. 523- 527. August, 1992. ISSN: 0018-9456. DOI: 10.1109/19.155919.
[14] N. R. Noroña Lucero, "Diagnóstico de perturbaciones armónicas en el Sistema Nacional Interconectado," tesis de grado, Ingeniería Eléctrica, Escuela Politécnica Nacional, Quito, Ecuador, 2011.
[15] C. A. Ríos Porras, M. Aristizabal Naranjo, and R. A. Gallego, "Análisis de armónicos en sistemas eléctricos," Sci. Tech., vol. 1, no. 21, pp. 21-26, julio 2003.
[16] IEEE Guide for application and specification of harmonics filters, IEEE standard 1531-2003, 2003.
[17] H. Alvarado Perusquia, and J. M. Ramírez Sánchez "Metodología para el análisis de propagación y filtrado de armónicas en sistemas eléctricos," tesis de licenciatura, Ingeniería Eléctrica, Instituto Politécnico Nacional, Ciudad de México, México, 2010. [en línea]. Disponible en: http://tesis.ipn.mx/jspui/bitstream/123456789/6514/1/METODOLOGANALIS.pdf.
[18] E. Parra, Análisis de armónicos en sistemas de distribución. Bogotá: Unibiblos, 2004. XM SA ESP, Descripción del Sistema Eléctrico Colombiano, 2015 [en línea]. Disponible en: http://www.xm.com.co/Pages/DescripciondelSistema Electrico colombiano. aspx.
[19] Schneider Electric, Capítulo M. Detección y filtrado de armónicos, 2015. [en línea]. Disponible en: http://www.schneiderelectric.es/documents/local/productosservicios/distribucion_electrica/guia_instalaciones_electricas/capitulo-m-deteccion-filtrado-armonicos .pdf.
[20] Circutor SA, ¿Vale cualquier banco de capacitores?, 2015. [en línea]. Disponible en: http://circutor.es/es/documentacion/articulos/833-vale-cualquier-bateriade-condensadores.

Biographies

Emmanuel Hernandez (S'09) received the Graduation degree from the Instituto Tecnológico de Orizaba, Veracruz, México, in 2008, and the M.Sc. degree in electrical engineering in 2010 from the Instituto Tecnológico de Morelia, Michoacán, México, where he is currently working toward the Ph.D. degree. His areas of interest include power quality and harmonic analysis.

Reynaldo Iracheta completed his studies in Mechanical and Electrical Engineering (2003) and Master's Degree in Electrical Engineering (2007) in the Autonomous Univer-sity of Nuevo Leon. He completed his Doctor grade in the Specialty of Electrical Engineering in (CINVESTAV) in 2013. Actually, he works in the Management of Industrial Mathematics in CIMAT.

Miguel Á. Hernández completed his undergraduate studies in Computer Engineering, at the National Autonomous University of Mexico. He completed his master's and doctoral studies in electrical engineering in the area of control and automation at the National Autonomous University of Mexico. His current lines of research are: Simulation of virtual reality systems, development of low power wind turbine prototypes, control of the power generation system and applications in renewable energies.